Maximum Annually Recurring Wave Heights in Hawai'i[1]

Sean Vitousek[2,3] *and Charles H. Fletcher*[2]

Abstract: The goal of this study was to determine the maximum annually recurring wave height approaching Hawai'i. The motivation was scientific as well as administrative: to enhance understanding of the recurring nature of dominant swell events, as well as to inform the Hawai'i administrative process of determining the "upper reaches of the wash of the waves" (Hawai'i Revised Statutes [H.R.S.] § 205-A), which delineates the shoreline. We tested three approaches to determine the maximum annually recurring wave, including log-normal and extremal exceedance probability models and Generalized Extreme Value (GEV) analysis using 25 yr of buoy data and long-term wave hindcasts. The annual recurring significant wave height was found to be 7.7 ± 0.28 m (25 ft ± 0.9 ft), and the top 10% and 1% wave heights during this annual swell was 9.8 ± 0.35 m (32.1 ft ± 1.15 ft) and 12.9 ± 0.47 m (42.3 ft ± 1.5 ft), respectively, for open North and Northwest Pacific swell. Directional annual wave heights were also determined by applying hindcasted swell direction to observed buoy data lacking directional information.

The islands of Hawai'i lie in the midst of a large swell-generating basin, the North Pacific. Tropical storms tracking to the northwest and north of the Islands produce winter swell with breaking face heights exceeding 5 m several times each year. These swell events lead to concerns over coastal erosion, coastal flooding, and water safety for the large population of ocean communities in Hawai'i. Runup generated by the largest of these waves poses a hazard to coastal development by flooding roadways, undermining structures, and causing erosion. According to Hawai'i state law (Hawai'i Revised Statutes [H.R.S.] § 205-A) the highest runup of these annual swells sets the legal position of the shoreline.

In Hawai'i, the shoreline serves as a reference line used to delineate public beach access, construction setbacks, state conservation land, submerged lands, and the border of management jurisdiction. Several states define the shoreline differently; for example, California uses the mean high water mark and Massachusetts uses the mean low water mark based on tidal water levels (not including wave setup or runup). In 1968, the State of Hawai'i changed the definition of the shoreline from the mean high water mark to the highest reach of the waves (*Ashford v. State of Hawai'i*). The State of Hawai'i definition of the shoreline is "the upper reaches of the wash of the waves, other than storm and seismic waves, at high tide during the season of the year in which the highest wash of the waves occurs, usually evidenced by the edge of vegetation growth, or the upper limit of debris left by the wash of the waves" (H.R.S. § 205-A). In October 2006, the Hawai'i Su-

[1] This paper is funded by a grant/cooperative agreement from the National Oceanic and Atmospheric Administration, Project No. R/EP-26, which is sponsored by the University of Hawai'i Sea Grant College Program, SOEST, under Institutional Grant No. NA05OAR4171048 from NOAA Office of Sea Grant, Department of Commerce. The views expressed herein are those of the authors and do not necessarily reflect the views of NOAA or any of its subagencies. UNIHI-SEAGRANT-JC-06-17. Manuscript accepted 28 November 2007.

[2] Coastal Geology Group, Department of Geology and Geophysics, School of Ocean and Earth Science and Technology, University of Hawai'i at Mānoa, 1680 East-West Road, POST 721, Honolulu, Hawai'i 96822.

[3] Corresponding author (e-mail: seanfkv@hawaii.edu).

Pacific Science (2008), vol. 62, no. 4:541–553

preme Court issued a ruling (*Diamond v. State of Hawai'i*) that the shoreline should be established "at the highest reach of the highest wash of the waves."

The State of Hawai'i has established a coastal management system that relies on this definition of the shoreline, not only as a demarcation of public shoreline access, but also to establish a baseline for construction control and development setbacks. The discord of private landowners seeking to preserve or develop the economic value of their property and public ocean users wishing to access and preserve pristine coastal environments is responsible for continuing debate over shoreline laws. Resolving the annually recurring maximum wave height around the Islands would improve the scientific basis to understanding the shoreline definition, because this line is set by the upper limit of wave runup resulting from the largest or set of largest annually recurring waves (under optimal runup conditions). Runup is not a simple function of wave height; rather the interaction of different wave conditions and topography determine runup. However, wave height is a fundamental determinant of runup; contrary to topography, which is fixed as a data set, wave height is not. This paper provides the description of maximum annually recurring wave heights in Hawai'i for such purpose.

Local consulting engineers as part of their respective design projects on the coast are required to describe the regional and local wave climate. This analysis typically consists of specifying the largest characteristic ranges and scatter tables or rose diagrams of wave height, period, and direction of the dominant swell regime for the area of interest. Such engineering reports (e.g., Noda and Associates 1991, Bodge and Sullivan 1999, Bodge 2000) do not give detailed statistical analyses of the recurring nature of swells in Hawai'i.

To provide a comprehensive analysis, we wish to resolve the annually recurring maximum wave based on the best records and state-of-the-art methods. The determination of the annually recurring wave height is also the first step to ensuring a sound scientific basis for policy-based decision making involved in the determination of the shoreline as defined by H.R.S. § 205-A.

Previous Work

The seasonal wave cycle in Hawai'i has been explored in several different publications. Moberly and Chamberlain (1964) outlined the wave cycle in terms of four swell regimes: North Pacific swell, northeast trade wind waves, Kona storm waves, and southern swell. We have added a wave rose to their original graphic depicting annual swell heights and directions (Plate 1).

The seasonal wave cycle in Hawai'i is characterized by large North Pacific swell and decreased trade wind waves dominating in winter months and southern swell accompanied by increasing trade wind waves dominating in summer months. However, large-scale oceanic and atmospheric phenomena including El Niño Southern Oscillation (ENSO) and Pacific Decadal Oscillation (PDO) are thought to control the number and extent of extreme swell events (Seymour et al. 1984, Caldwell 1992, Inman and Jenkins 1997, Seymour 1998, Allan and Komar 2000, Wang and Swail 2001). Extreme wave events have been argued to control processes such as coral development (Dollar and Tribble 1993, Rooney et al. 2004) and beach morphology (Moberly and Chamberlain 1964, Ruggiero et al. 1997, Storlazzi and Griggs 2000).

Although there are several factors that contribute to annual variability in maximum wave height in Hawai'i, including the ENSO and PDO cycles, we seek to resolve the mean maximum annual signal from both highs and lows of these cycles. Ruggiero et al. (1997) evaluated extreme runup using empirical equations as a means of calculating frequency of dune impact. This empirical approach or a more robust process-based numerical modeling approach could similarly be used to evaluate the extent of extreme runup in Hawai'i based on the annual maximum wave height. This study could provide boundary conditions for a more sophisticated wave transformation and runup model for identification of the shoreline in Hawai'i for a particular location.

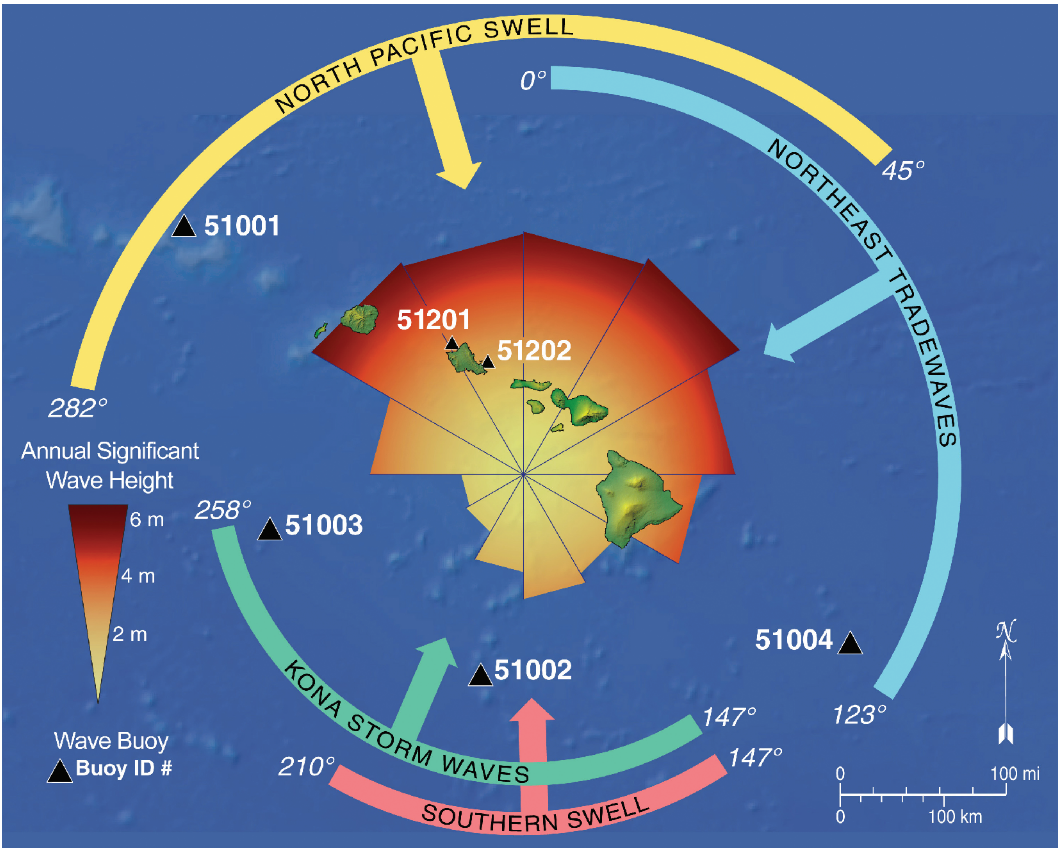

PLATE 1. Hawai'i dominant swell regimes after Moberly and Chamberlain (1964), and wave-monitoring buoy locations.

MATERIALS AND METHODS

To determine the annually recurring maximum wave height we used the record of wave buoys from the National Oceanic and Atmospheric Administration (NOAA) National Data Buoy Center (NDBC) and WaveWatch III (WWIII) model hindcasts from the Coastal and Hydraulics Laboratory's (CHL) Wave Information Studies (WIS) program (Vicksburg, Mississippi).

Hourly reports of significant wave height (average of the largest one-third of wave heights, H_s) and other meteorological information from monitoring buoys are available from NOAA's NDBC Web site (http://www.ndbc.noaa.gov/Maps/Hawaii.shtml). Based on the observation that wave heights follow a Rayleigh distribution, we can use the significant wave height to estimate other statistics of a swell, such as the mean wave height or the top 10% wave height, based on the significant wave height. These buoys have an instrument precision of 0.2 m, which results in small errors (less than 5% for all waves above 4 m).

Our focus concerned buoy 51001 (buoy 1), which is located 315 km northwest of the island of Kaua'i and is moored at a depth of 3.25 km. The buoy has recorded 25 yr of wave height and period data, since 1981.

Buoy 1 is ideally located to record North and Northwest Pacific swell without interference from neighboring islands. Only recently has buoy 1 been able to record swell direction. Thus the time series recorded in the majority of buoy 1 data and by all of the remaining buoys lack swell direction. The lack of observations of wave direction means that any analysis of open North Pacific and Northwest Pacific swell is limited to data from buoy 1 because all the remaining buoys are significantly affected by island blockage. However, hindcasts using WaveWatch III can be used to recover directional information.

Long-term statistical analysis was applied to the simple case of the 1-yr recurring significant swell height. Statistics of extremes can usually be extrapolated to approximately three times the length of the time series. Because we were primarily interested in the annually recurring maximum wave height, our 25-yr time series was more than adequate to resolve this value. Long-term statistical models are typically applied to long-return-period events such as the 50- to 100-yr events; such methods were originally developed to define stream flood heights or return periods from discharge records (Gumbel 1941). Although typically applied to long-return periods, they can also be applied for short- and intermediate-return periods. The following procedure was used to construct our long-term statistical model:

(1) Large swell events (n per year) from the buoy record were assigned an exceedance probability (see equation).
(2) Log-normal and extremal models used linear regressions to determine the relationship between large swell events and exceedance probability (the probability that a larger swell event will occur during the return period). To corroborate this analysis Generalized Extreme Value (GEV) probability models also determined the relationship between large swell events and exceedance probability using Maximum Likelihood Estimates (MLE).
(3) Methods including removing outliers and the peak over threshold (van Vledder et al. 1993) method were evaluated to improve model performance.
(4) These statistical models assigned probabilities to a full range of swell heights and were modified to give the relationship between swell heights and return period (particularly the 1-yr return period).
(5) The maximum annually recurring wave height is determined from the tail of a Rayleigh distribution.

The log-normal statistical model was constructed on the assumption that maximum swell events will plot as a linear function on a horizontal logarithmic scale of exceedance probability. Exceedance probability ($Q = 1 - p$) was given by the probability that the next swell will be greater than the sorted

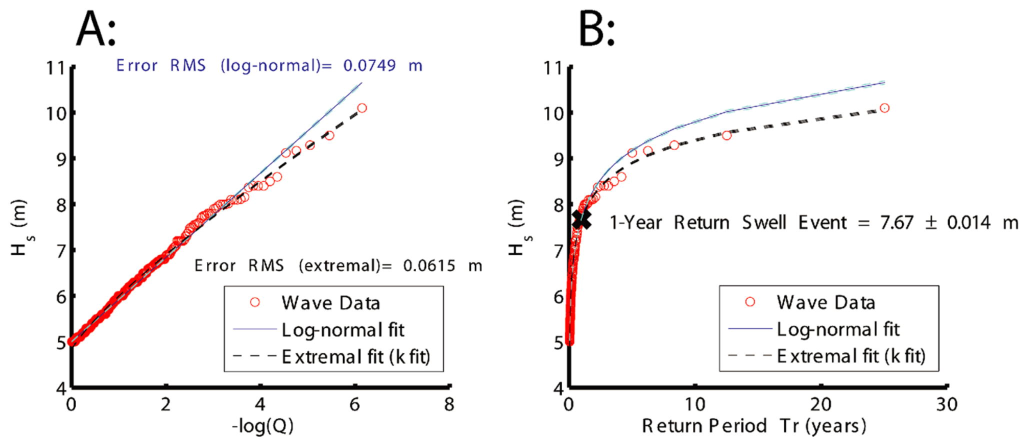

FIGURE 1. Log-normal and extremal probability models for the top 70 largest wave height events per year recorded by buoy 1. The largest wave heights recorded by buoy 1 are plotted versus the negative log of exceedance probability in (*A*) and plotted versus the return period in (*B*). In these models the largest event (a 12.3 m significant wave height) outlier has been removed and the peak over threshold method is used with a threshold of 5 m.

wave events on record as if drawing from a hat containing all the maximum swell heights and the next swell event.

Wave Height	Q = Exceedance probability = $(1 - p)$
$H_{s1} \rightarrow$	$\frac{N}{N+1}$ ← High probability the next swell will be larger.
$H_{s2} \rightarrow$	$\frac{N-1}{N+1}$
H_{s3}	$\frac{N-2}{N+1}$
⋮	⋮
$H_{sN} \rightarrow$	$\frac{1}{N+1}$ ← Low probability the next swell will be larger.

In this procedure, H_{s1} is the smallest significant wave height, H_{sN} is the largest significant wave height, and N is the total number of waves in the analysis. Selecting different numbers of events (n) per year, such as the single maximum significant wave height each year or the top 25 significant wave heights, can yield different results as discussed later.

Our long-term statistical analyses were performed using the significant wave height. To determine the maximum wave height that occurs with a given significant wave height requires further statistical analysis on a probability distribution of random waves.

RESULTS

Our results fell into two categories: results using the log-normal and extremal exceedance probability models and results using the GEV models.

Log-Normal and Extremal Models

The log-normal model of exceedance probability versus wave height, as seen in Figure 1, is quite linear on a log (x-axis)-linear (y-axis) scale.

Figure 1*A* shows a log-normal model of the data, with the following equation:

$$H_s = A[-\log Q] + B$$

where A and B are regression coefficients.

An extremal model of the same data is shown in Figure 1*A* and uses the following equation, which differs from the log-normal model by the $1/k$ exponent term (below), which serves to limit the occurrence of extremely large events (when $k > 1$) and give a better fit:

$$H_s = A[-\log Q]^{1/k} + B$$

Figure 1*B* shows the same data in terms of significant wave height versus return period instead of exceedance probability. This allows determination of the annually recurring significant wave height. The relationship between the exceedance probability (Q) and the return period (T_R) is

$$T_R = \frac{r.i.}{Q}$$

where $r.i.$ is the recurrence interval.

The return period is simply the recurrence interval, $r.i.$ (1/70 yr because we used the top 70 events each year) divided by the exceedance probability (Q). In this case 70 events was the smallest number of recorded wave heights in a year of buoy data, because the buoy was not operating for the majority of 1983 due to maintenance issues.

The 1-yr return period is given in Figure 1*B* as 7.67 ± 0.014 m. The confidence levels, CI, shown in Figure 1*A* and *B* are given by the typical confidence interval equations for a linear regression:

$$CI = t_{N-2,1-\alpha/2}(SE)\sqrt{\frac{1}{N} + \frac{(x-\mu)^2}{\sum(x-\mu)^2}}$$

where t is given by the student-t statistic, α is the significance level, μ is the mean, and SE is the standard error given by the equation

$$SE = \sqrt{\frac{1}{N-2}\sum(y-\hat{y})^2}$$

This 1-yr return swell event has an annual return probability percentage based on the recurrence interval of the time series given by the equation:

$$E = 1 - \left(1 - \frac{r.i.}{T_R}\right)^{(L/r.i.)}$$

where E is the probability that we will encounter the event (= 64% for the following conditions), $r.i.$ is the recurrence interval (1/70 yr), T_R is the return period (1 yr), and L is the life span (1 yr). According to the buoy 1 time series, significant wave heights exceeding 7.7 m have occurred in 16 of the 25 yr on record (i.e., 68% of the time, which is consistent with the encounter probability of 64% calculated earlier).

Log-normal models tend to overpredict large events because physical processes exert natural limitations on event magnitude that are not accounted for in the model. For example, flood height is limited by the rainfall amount, wave height is limited by energy dissipation, and hurricane intensity is limited by heat transfer to fuel propagation. Thus, extreme events (long-return-period events) are often not best fit with a log-normal relationship, and other models such as the extremal model should be considered. A particular example of this concerns the largest significant wave height in the 25-yr record of buoy 1: a 12.3 m event that occurred at 0400 hours on 5 November 1988. The second largest on record is 10.1 m (1985). These are the only two events with significant wave heights exceeding 10 m and, notably, the largest swell on record is more than 2 m greater than the next largest swell. In the analysis just described this 12.3 m event was removed. We must consider the possibility that the 12.3 m significant wave height event was an extraordinary swell and perhaps unlikely to occur during a period of 25 yr. In exceedance probability models the largest event (12.3 m) provides information about the longest return period of recorded data (25 yr in this case). In reality, this 12.3 m event could very well be the 50- or 100-yr swell event, and including this event overestimates the frequency of large events in the model as well as affects the value for the annually recurring wave height. A simple procedure is to test potential overestimation to determine the best fit *without* the outlier event and determine the expected return period of the removed outlier. Using the model described earlier, the return period of a 12.3 m event is approximately 150 and 700 yr using log-normal and extremal models, respectively. Typically, forecasts longer than three to four times the data collection period (25 yr in this case) are not realistic, and furthermore they are not the focus of this paper. However, we performed such analysis to confirm our suspicion that a very large event occurred in 1988 with a recur-

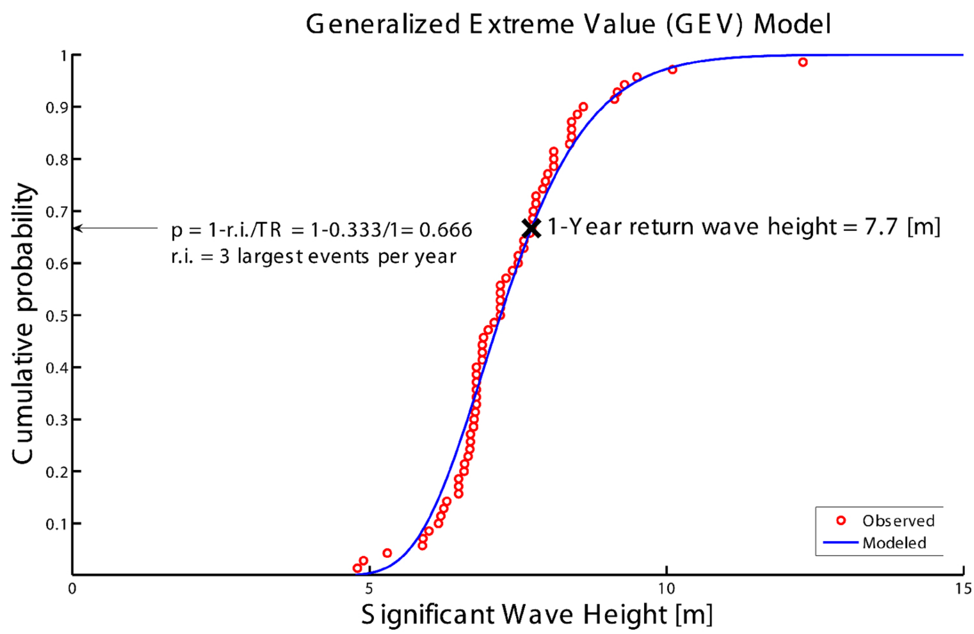

Figure 2. The Generalized Extreme Value probability model used to determine the annually recurring significant wave height.

rence interval exceeding 100 yr and justify its removal from the analysis.

Returning to the annual return period, a log-normal model would perhaps be appropriate, but for completeness we investigated the behavior of swell events using both log-normal and extremal models as well as the GEV model (described next). The GEV statistical model returns results very similar to those of the log-normal and extremal models, which focus on our estimates of the annually recurring significant wave height.

Generalized Extreme Value (GEV) Model

The GEV distribution is applied to determine relationships between wave height and return period with particular focus on the annually recurring wave height. Introduced by Jenkinson (1955), the GEV distribution uses Gumbel (type I), Frechet (type II), and Weibull (type III) distributions for different values of the shape parameter, $\kappa = 0$, $\kappa < 0$, $\kappa > 0$, respectively. Iterative maximum-likelihood estimates (MLE) fit the observed data to find the best estimates of the shape (κ), scale (σ), and location (μ) parameters of the GEV cumulative distribution function, $F(x)$, given by:

$$F(x) = \exp\left\{-\left[1+\kappa\left(\frac{x-\mu}{\sigma}\right)\right]^{-1/\kappa}\right\} \quad \text{for } \kappa \neq 0$$

$$\exp\left\{-\exp\left[-\frac{(x-\mu)}{\sigma}\right]\right\} \quad \text{for } \kappa = 0$$

Based on given probability distributions and the return period probability equation $p_{T_R} = 1 - \frac{r.i.}{T_R}$, wave height for an arbitrary return period is found. The GEV model is more robust than the previous approach because it combines the Gumbel, Frechet, and Weibull extreme value distributions, although it yields very similar results to our log-normal and extremal analysis (Figure 2). The GEV analysis, being a more robust model, remains largely unaffected by the presence of the 12.3 m event.

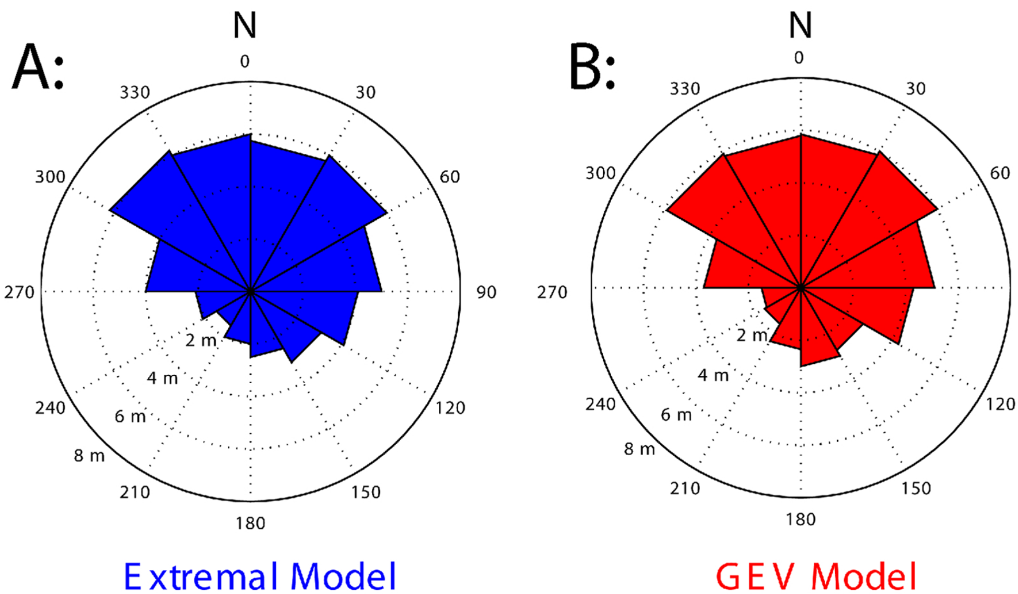

FIGURE 3. Observed directional annually recurring maximum significant wave heights (H_s) given from (*A*) extremal and (*B*) GEV models.

Recovering Swell Directionality from Model Hindcasts

Thus far the annually recurring wave height analysis is applicable to open North and Northwest Pacific swells because no information of wave direction has been considered. By using WaveWatch III (WWIII) model hindcasts concurrent with buoy data to recover the directionality of wave heights, we can determine the annually recurring maximum wave heights for a particular direction window. WWIII is an ocean-scale spectral wave model on a 0.5-degree grid that computes open swell generation and propagation based on spatial wind fields. WWIII has been well validated using buoy and altimetry data (Tolman 2002, Baird and Associates 2005, Tracy et al. 2006). Figure 3 and Table 1 show the annually recurring maximum significant wave heights according to buoy data for extremal and GEV models for swell direction windows of 30 degrees. Applying modeled direction to the actual buoy data may seem problematic, but it is the best option to ensure preference toward observed over-modeled wave height. As can be seen from Figure 3, observed directional annually recurring maximum significant wave heights produced by both models are similar as are results from the observed versus modeled wave heights shown in Table 1.

The north to northwest windowed annual significant wave heights found in Table 1 are smaller than the previously determined value of 7.7 m because the largest events used in the analysis do not fall into the same 30-degree windows. This limiting effect is caused by the directional variability of north swells, which typically range clockwise from 270 to 90 degrees (W–E). Analysis of all northern-facing swell directions (270 to 90 degrees) recovered this 7.7 m annual wave height. Southern swell occurs in much more narrow-banded directions, typically ranging clockwise from 150 to 210 degrees (SSE–SSW) and therefore should be much less affected by the limiting effect of the directional variability.

Significant Wave Height versus Maximum Probable Wave Height

It is important to keep in mind that 7.7 m is the annually recurring *significant wave height*

TABLE 1

Observed and Modeled Directional Annually Recurring Maximum Significant Wave Heights Using Extremal and GEV Exceedance Probability Models

Window			Annual H_s (m): Extremal Model		Annual H_s (m): GEV Model	
Lower	Upper	Source	Observed	Modeled	Observed	Modeled
0	30	Buoy1	5.75	6.1	5.85	6.15
30	60	Buoy1	6	6.5	6	6.45
60	90	Buoy4	5	5.25	5.1	5.37
90	120	Buoy4	4.1	4.2	4.3	4.32
120	150	Buoy4	3.1	3.1	2.75	2.65
150	180	Buoy2	2.5	2.4	3	2.95
180	210	Buoy2	2	2.1	2.35	2.35
210	240	Buoy1	1.5	1.5	1.6	1.65
240	270	Buoy1	2.1	2.2	1.5	1.6
270	300	Buoy1	4	4.5	3.7	3.9
300	330	Buoy1	6.2	6.7	5.9	6.4
330	360	Buoy1	6	6.5	5.8	6.2

Note: Wave hindcasts of buoy 3 did not return more than one swell event per year in the southerly and westerly directional windows; hence buoy 1 was used instead.

or the average of the highest one-third of the wave heights. Each wave height data point from the buoy record used in the analysis was part of a swell train that certainly contained larger waves. The significant wave height represents the typical observational state of the ocean, not the very largest waves that occur during a swell event. To determine the largest 10% and 1% of wave heights, we assumed that the probability distribution of the waves followed a Rayleigh distribution, which has the following probability distribution function (pdf):

$$p(H) = \frac{2H}{H_{rms}^2} \exp\left[-\left(\frac{H}{H_{rms}}\right)^2\right]$$

where $p(H)$ is the probability of encountering a wave of a given height, H, and H_{rms} is the root mean square wave height, which is equal to $H_s/\sqrt{2}$.

The assumption that random waves follow a Rayleigh distribution has been shown to be quite good for deep-water waves with a narrow-banded wave spectrum (Longuet-Higgins 1952) (i.e., waves created by a single swell event rather than two converging swell events). With a given pdf, one can determine several parameters of interest, such as the average of the 10% largest waves or the maximum probable wave. Maximum probable wave, H_{max}, can be solved using the following equation:

$$\int_{H_{max}}^{\infty} p(H)\, dH = 1/N$$

where N is the number of waves in the swell event. Solving for H_{max} yields the following equation:

$$H_{max} = H_{rms}\sqrt{\ln N} = H_s\sqrt{\frac{1}{2}\ln N}$$

The average of the 10% largest waves is given by the following equation:

$$\text{Avg. of } H_{10\%} = \frac{\int_{H_{10\%}}^{\infty} p(H)H\, dH}{\int_{H_{10\%}}^{\infty} p(H)\, dH}$$

or more generally,

$$\text{Avg. of } H_{pct\%} = \frac{\int_{H_{pct\%}}^{\infty} p(H)H\, dH}{\int_{H_{pct\%}}^{\infty} p(H)\, dH}$$

where $H_{10\%}$ or $(H_{pct\%})$ is given by the equation: $H_s\sqrt{\frac{1}{2}\ln\frac{1}{pct}}$, where pct is the percentage

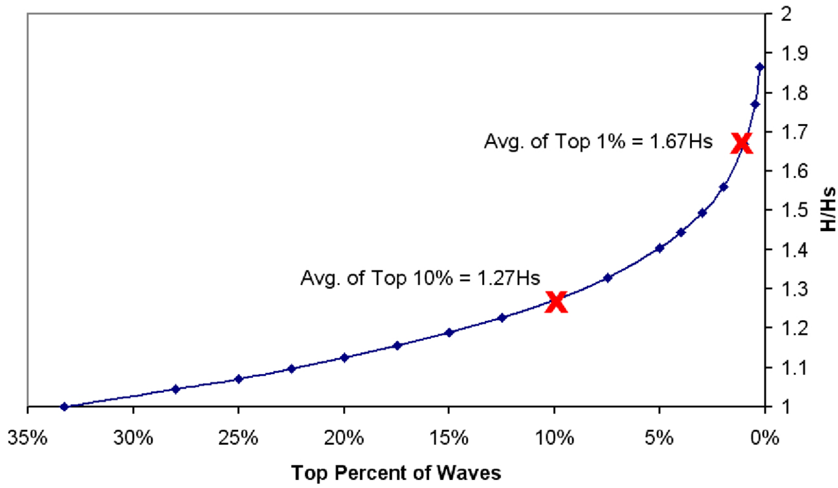

FIGURE 4. Top percentage of waves versus relation to significant wave height (H_s).

of interest. By integrating the equation just given, the averages of the top percentages of wave heights in relation to the significant wave height are shown in Figure 4.

Consistently, according to the Coastal Engineering Manual (U.S. Army Corps of Engineers 2002), the average of the largest 10% and 1% of wave heights in a swell event is given by the following:

$$H_{10\%\ \text{highest}} = 1.27H_s = 9.8\ \text{m}$$
$$H_{1\%\ \text{highest}} = 1.67H_s = 12.9\ \text{m}$$
$$H_{\max} = 1.86H_s = 14.3\ \text{m}$$

This analysis, for $H_{\max}$, is based on 1,000 waves and represents wave conditions that would occur for a peak swell duration of around 4.44 hr assuming the typical wave period is 16 sec. Note: Wave hindcasts of buoy 3 did not return more than one swell event per year in the southerly and westerly directional windows; hence buoy 1 was used instead.

Table 2 shows the maximum annually recurring significant wave heights and the largest 10% and 1% wave heights for various directions in 30-degree windows around Hawai‘i.

TABLE 2

Observed Maximum Annually Recurring Significant Wave Heights and the Largest 10% and 1% Wave Heights for Various Directions around Hawai‘i

Window		Annual H_s (m): GEV Model		
Lower	Upper	Observed-H_s	$H_{1/10}$	$H_{1/100}$
0	30	5.9	7.4	9.8
30	60	6.0	7.6	10.0
60	90	5.1	6.5	8.5
90	120	4.3	5.5	7.2
120	150	2.8	3.5	4.6
150	180	3.0	3.8	5.0
180	210	2.4	3.0	3.9
210	240	1.6	2.0	2.7
240	270	1.5	1.9	2.5
270	300	3.7	4.7	6.2
300	330	5.9	7.5	9.9
330	360	5.8	7.4	9.7

DISCUSSION

The number of maximum swell events (three per year versus some other number) used in the exceedance probability model influences the determination of the annually recurring significant wave height. This motivates a sensitivity test to determine the optimal number of events to use. Notably, as more events are selected per year the annual recurring wave

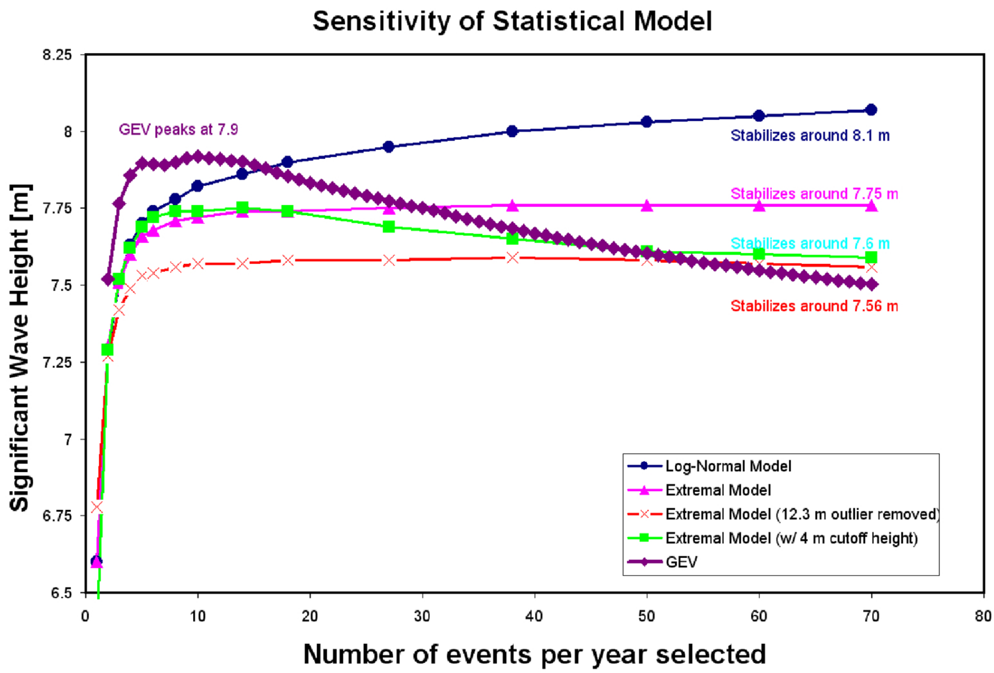

FIGURE 5. Sensitivity of models to number of largest events selected per year.

height is higher for the log-normal and extremal models and lower for the GEV model after a peak at about 10 events per year. However when large numbers of events are selected ($N > 10$) the return wave height prediction for the log-normal and extremal models begins to stabilize (Figure 5).

This increasing annual recurring wave height result for the log-normal and extremal models is due to the trend that as more events are selected per year, the data become saturated with lower swell events, which tend to dominate the behavior of the regression. Because a majority of data points behave with a return period of less than 1 yr, the log-normal model predominantly captures the behavior of the frequency of short-return-period events at the expense of long-period data. This can be seen in Figure 6: the log-normal fit is quite good for short-return-period data and problematic for long-return-period data.

As seen in Figure 6*A* a large number of short-return-period (high exceedance probability) data points force the slope of the log-normal fit to be higher than it would be for long-return-period data points, which seem to have a lower slope. This suggests that the inherent behavior or occurrence of short-return-period events differs from that of long-return-period events, and thus the entire data set is not appropriately represented by a log-linear model.

In dealing with estimates of the annually recurring significant wave height, it is somewhat unrealistic to give a confidence level on the order of centimeters when dealing with waves exceeding 7 m, although by this analysis it may be statistically acceptable to do so. Rather, we make a recommendation that accounts for the variability by using different numbers of events selected each year that typically range ± 0.2 m and the instrument precision, which is also ± 0.2 m. Summing the error in quadrature gives a confidence level of 0.28 m and still represents a very

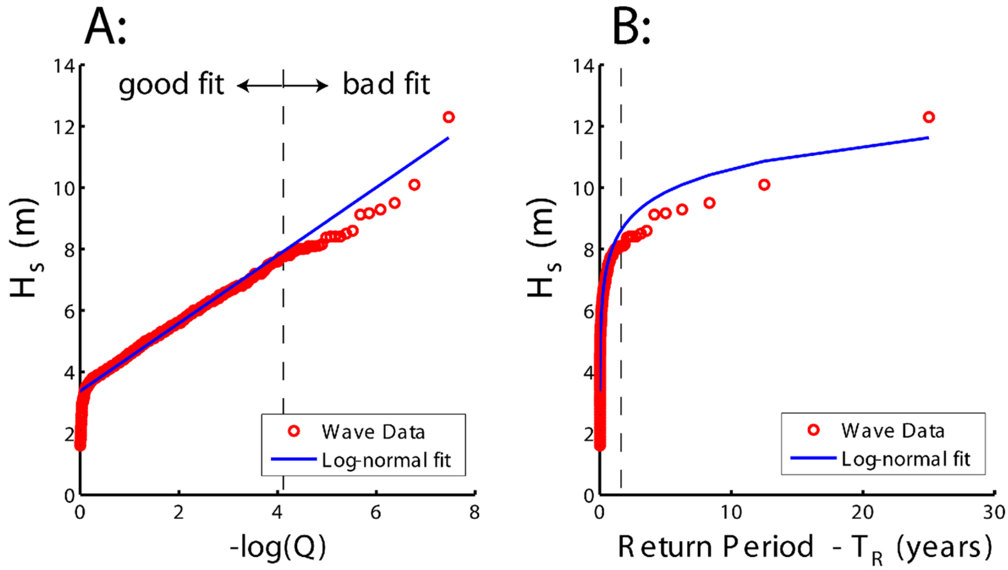

FIGURE 6. When a large number of events are used in analysis, the log-normal model is strongly fit to the high-frequency events (which represent the bulk of the data) at the expense of the extreme events. The fit of the wave heights versus the negative log of exceedance probability is shown in (*A*), and the fit of wave heights versus the return period is shown in (*B*).

narrow band of about 3.5% of the wave height.

Thus our recommendation for the annually recurring significant wave height in Hawai'i is 7.7 ± 0.28 m (25 ft ± 0.9 ft), and the top 10% and 1% wave heights during this annual swell are 9.8 ± 0.35 m (32.1 ft ± 1.15 ft) and 12.9 ± 0.47 m (42.3 ft ± 1.5 ft), respectively. For good measure we also multiply the confidence level by the coefficient given on the y-axis of Figure 4, so that the confidence levels represent the same percentage of the final value. The difference between selecting the annually recurring significant wave height as 7.5 or 7.7 or somewhere in between is fairly trivial, especially for engineering calculations, because the difference between selecting one or the other results in a maximum difference of only 3.5%.

It is important to note that this analysis considers only deep-water wave heights, which are not the same as wave heights near the shoreline. There are several physical processes that can cause deep-water wave heights to increase or decrease when propagating into shallower water, such as shoaling, refraction, diffraction, and nonlinear interactions. There are a number of theories and methods that are used to model the transformation from deep-water wave heights to nearshore wave heights, including linear wave theory, spectral and phase-resolving wave models, and empirical equations. Caldwell (2005) applied this approach for predicting the observed breaking wave height at Waimea Bay, Hawai'i, from the deep-water wave height recorded by buoy 1.

It is also important to keep in mind that H_{max} represents the single largest wave that would occur during a swell event, and perhaps the 10% or 1% highest wave conditions (depending on the acceptable risk tolerance) would be more representative of all of the largest waves in a swell event. Another benefit of using the top 10% or 1% of wave heights is that information about the number of waves in a particular swell is not required. The analysis performed in Figure 4 has no input on the number of waves in a swell event; only the maximum probable wave requires the number of waves as input. These values should be considered the maximum annually recurring wave height for open north- and northwest-facing shores such as Kaua'i and O'ahu, where swell is directly incident to the shoreline and blocking from neighboring islands is minimized. For shorelines not directly exposed to North and Northwest Pacific swell the annually recurring maximum wave height may be estimated from Figure 3 or Table 1 and the relationship of H_s to H_{max} given in Figure 4 or Table 2.

Future Work

The determination of the maximum annually recurring wave height is just the first step in a process of formulating a sound scientific basis to evaluate the physical processes involved in wave runup. The next step in the process involves propagation of this deep-water wave into the nearshore and resolving the spatial variability of wave heights due to shoaling, refraction, diffraction, convergence, divergence, nonlinear interactions, and breaking. The spatial and physical properties of nearshore waves can be determined through modeling or empirical approaches. Finally, to evaluate runup, these nearshore wave properties can be used as boundary conditions in a runup model, and observations of runup should be recorded during wave events with deep-water wave heights around the annually recurring maximum level.

Literature Cited

Allan, J., and P. Komar. 2000. Are ocean wave heights increasing in the eastern North Pacific? Eos 81:561–567.

Baird and Associates. 2005. Pacific Ocean wave information study validation of wave model: Results against satellite altimeter data. Prepared for U.S. Army Corps of Engineers Engineering Research and Development Center, Vicksburg, Mississippi.

Bodge, K. R. 2000. Independent evaluation study of proposed Kuhio beach improvements. Prepared for State of Hawai'i, Department of Land and Natural Resources, Honolulu.

Bodge, K. R., and S. Sullivan. 1999. Hawaii pilot beach restoration project: Coastal engineering investigation. Prepared for State of Hawai'i, Department of Land and Natural Resources, Honolulu.

Caldwell, P. 1992. Surfing the El Niño. Mariners Weather Log 36:60–64.

———. 2005. Validity of North Shore, Oahu, Hawaiian Islands surf observations. J. Coastal Res. 21:1127–1138.

Dollar, S. J., and G. W. Tribble. 1993. Recurrent storm disturbance and recovery: A long-term study of coral communities in Hawaii. Coral Reefs 12:223–233.

Gumbel, E. J. 1941. The return period of flood flows. Ann. Math. Stat. 12:163–190.

Inman, D. L., and S. A. Jenkins. 1997. Changing wave climate and littoral drift along the California coast. Pages 314–327 *in* O. T. Magoon, ed. Proceedings of the California and the World Ocean Conference '97 Conference. American Society of Civil Engineers, San Diego.

Jenkinson, A. F. 1955. The frequency distribution of the annual maximum (or minimum) values of meteorological elements. Q. J. R. Meteorol. Soc. 81:158–171.

Longuet-Higgins, M. S. 1952. On the statistical distribution of the wave heights of sea waves. J. Mar. Res. 11:245–266.

Moberly, R., and T. Chamberlain. 1964. Hawaiian beach systems. Hawai'i Institute of Geophysics Report 64-2, University of Hawai'i at Mānoa, Honolulu.

Noda, E. K., and Associates. 1991. Wave measurement program: Offshore Waikiki Beach. Prepared for State of Hawai'i, Department of Land and Natural Resources, Honolulu.

Rooney, J., C. Fletcher, E. Grossman, M. Engels, and M. Field. 2004. El Niño influence on Holocene reef accretion in Hawai'i. Pac. Sci. 58:305–324.

Ruggiero, P., G. M. Kaminsky, P. D. Komar, and W. G. McDougal. 1997. Extreme waves and coastal erosion in the Pacific

Northwest: Ocean wave measurements and analysis. Pages 947–961 *in* Proceedings of the 3rd International Symposium on Ocean Wave Measurement and Analysis. American Society of Civil Engineers, Virginia Beach, Virginia.

Seymour, R. J. 1998. Effect of El Niños on West Coast wave climate. Shore & Beach 66:3–11.

Seymour, R. J., R. R. Strange III, D. R. Cayan, and R. A. Nathan. 1984. Influence of El Niños on California's wave climate. Pages 215–230 *in* B. L. Edge, ed. Proceedings of the 19th International Conference on Coastal Engineering. American Society of Civil Engineers, New York.

State of Hawai'i. 1968. Supreme Court of Hawai'i: Ashford v. State of Hawai'i. Hawai'i 314, 452, 440 P2d 76.

———. 2006. Board of Land and Natural Resources: Diamond v. State of Hawai'i. Hawai'i 161, 145 P3d 704.

Storlazzi, C. D., and G. B. Griggs. 2000. Influence of El Niño–Southern Oscillation (ENSO) events on the evolution of central California's shoreline. Geol. Soc. Am. Bull. 112:236–249.

Tolman, H. L. 2002. Validation of WAVEWATCH III version 1.15 for a global domain. NOAA/NWS/NCEP/OMB Tech. Note 213:33.

Tracy, B., J. Hanson, A. Cialone, H. L. Tolman, D. Scott, and R. Jensen. 2006. Hawaiian Islands severe wave climate 1995–2004. 9th Waves Workshop Program. 24–29 September, Victoria, British Columbia. American Society of Civil Engineers.

U.S. Army Corps of Engineers. 2002. Water wave mechanics. Coastal Engineering Manual II-1–74.

Van Vledder, G., Y. Goda, P. Hawkes, E. Mansard, M. J. Martin, M. Mathiesen, E. Peltier, and E. Thompson. 1993. Case studies of extreme wave analysis: A comparative analysis. Pages 978–992 *in* Proceedings, Waves 93, Ocean Wave Measurement and Analysis. American Society of Civil Engineers, New York.

Wang, S. L., and V. R. Swail. 2001. Changes of extreme wave heights in Northern Hemisphere oceans and related atmospheric circulation regimes. J. Clim. 14:2204–2221.